

Actin Filaments That Form Networks in Living Cells Fluctuate Rapidly and Independently of Each Other

Tomoteru Oka¹, Kouki Furukawa¹, Yasuyuki Oguma², Buntara Sthenly Gan³, Noriyuki Kataoka^{2,*}

¹Department of Mechanical Engineering, Graduate School of Engineering, Nihon University, Fukushima, Japan

²Department of Mechanical Engineering, College of Engineering, Nihon University, Fukushima, Japan

³Department of Architecture, College of Engineering, Nihon University, Fukushima, Japan

Email address:

kataoka.noriyuki@nihon-u.ac.jp (Noriyuki Kataoka)

*Corresponding author

To cite this article:

Tomoteru Oka, Kouki Furukawa, Yasuyuki Oguma, Buntara Sthenly Gan, Noriyuki Kataoka. Actin Filaments That Form Networks in Living Cells Fluctuate Rapidly and Independently of Each Other. *International Journal of Biomedical Science and Engineering*.

Vol. 11, No. 3, 2023, pp. 33-43. doi: 10.11648/j.ijbse.20231103.11

Received: August 28, 2023; **Accepted:** September 15, 2023; **Published:** September 27, 2023

Abstract: Actin filaments play a significant role in multiple essential cellular processes, including cell motility, vesicle and organelle movement, cell signaling, and cellular mechanosensing mechanisms. However, an important cellular processes, mechanosensing, remains debatable. This is because intracellular proteins such as actin filaments, focal adhesion complexes, and cell-nuclear junctions are dynamic structures that fluctuate minutely, although their binding is closely related to the mechanosensing mechanism. We established an original quasi-super-resolution image analysis method and revealed the existence of 3 Hz fluctuations in actin filaments in living cells at approximately 0.2 to 0.5 μm . We speculated that cells sense mechanical stresses such as fluid shear stress through the network structure of actin filaments and their connections to the substrate and cell nucleus. This study analyzed the fluctuations in actin filaments in the network structure of living cells using our quasi-super-resolution image analysis method under static culture conditions. In particular, we focused on the correlations between each actin fluctuation in the network structure. Fluorescence images showed that actin networks were well developed in the NIH3T3 cells. The maximum amplitude of actin filament fluctuations near the central region of the cell was 0.99 μm . Correlation coefficients of actin filament fluctuations in the network remained unchanged between the central and peripheral regions, with a maximum value of 0.23. These results suggested that actin filaments fluctuated independently within the network structure. Moreover, the distance between two actin filaments changed over time at the connecting point of the three actin filaments. These results suggest that strain occurs at the actin filament connecting points even when cells are under static culture conditions and that more complex mechanical states arise upon mechanical stimulation.

Keywords: Actin Filament, Fluctuation, Lifeact-GFP, Living Cell, Network Structure, Super-Resolution Technique

1. Introduction

Actin filaments in cells play various roles such as maintaining cell shape [1] and cell motility, and transmitting mechanical stimuli within cells [2]. Actin filaments form an intracellular cytoskeletal network structure by connecting focal adhesions of cells to substrates [3], intercellular adhesion, and linker of nucleoskeleton and cytoskeleton (LINC) complexes [4, 5] on the cell nucleus. Transduction of intracellular mechanical stress through the actin structure is involved in chromosome movement in the cell nucleus [6].

Moreover, inhibiting intracellular actin polymerization reduces the deformation of cell nuclei when cells are exposed to tensile stress [2]. To date, structural changes in F-actin in response to mechanical stimuli have been studied as static structures in fixed cells. However, living organisms effectively use the random movement of proteins on the cell membrane by Brownian motion [7] and the movement of green fluorescent proteins in the cytoplasm [8]. Based on these studies, we hypothesized that the actin filaments would also fluctuate. We observed real-time fluctuations in actin filaments in living cells and found that the frequency was

approximately 3 Hz and the amplitude of the fluctuations was approximately 0.2–0.3 μm , which is almost equal to the spatial resolution of a fluorescence microscope [9]. Therefore, we attempted to develop a quasi-super-resolution image analysis method to improve the resolution [9]. Kiuchi *et al.* proposed a super-resolution image analysis method to reconstruct an image of a single actin filament from fluorescent images captured over a long period [10]. In contrast, our quasi-super-resolution image analysis method produces an image with improved resolution from a single fluorescent image, enabling the rapid movement of actin filaments at approximately 10 fps.

Many cells such as vascular endothelial cells change their shape and function in response to fluid shear stress and stretch stimuli, and actin filaments play a major role in this sensing mechanism [11]. Because the binding of actin filaments to the cell nucleus or of actin filaments to the substrate [12], and the linking of intercellular binding sites [13], is considered important for sensing these mechanical stimuli, it is essential to observe the network structure of actin filaments in real time.

Thus, it is vital to analyze the mechanotransduction of actin filaments as dynamic structures in network structures and clarify the interrelationships of actin filaments within the network structures. This study visualized fluctuations in actin filaments as network structures in living cells using our own quasi-super-resolution image analysis method [9]. The correlation between the fluctuations in actin filaments in the network structure was analyzed. The mechanical condition of some actin filaments based on the results of the F-actin fluctuation analysis was considered. The relationship between the fluctuations obtained from this analysis was evaluated within a network constructed using attached actin filaments. The strain at the connecting point due to the actin filament fluctuation was analyzed with changes in the length of the observation points on the two actin filaments.

2. Method

2.1. Cell Culture

NIH3T3 cells were cultured to observe actin filament

fluctuations. NIH3T3 cells were cultured in high-glucose Dulbecco's modified Eagle's medium supplemented with 10% newborn calf serum and 1% penicillin-streptomycin. The cells were seeded in 0.1% gelatin-coated 25 cm^2 cell culture flasks. When the cells reached 80–90% confluence, they passed at a 1:4 ratio.

2.2. Visualization of Intracellular Actin Filaments

Actin filaments in living NIH3T3 were visualized using Lifeact-GFP. Lifeact-GFP was transfected using Lipofectamine 3000 (Thermo Fisher Scientific, MA, USA), according to the manufacturer's instructions. Transfected cells were selected using 50 mg/mL geneticin (Thermo Fisher Scientific) and seeded on gelatin-coated glass-bottomed cell culture dishes.

2.3. Observation of Intracellular Actin Filaments

When the cells reached confluence, the cell culture dish was placed in an incubator on the stage of an inverted microscope (IX70, Olympus, Tokyo, Japan). Actin filaments in living cells were observed using a x60 objective lens and confocal microscope (CSU10 Yokogawa, Tokyo, Japan) and CCD (ANDOR, Belfast, UK) connected to an inverted microscope. Actin filaments were excited by a 488 nm blue laser and were captured 0.1 s with a 70 ms exposure time.

2.4. Quasi-Super-Resolution Technique

Figure 1 illustrates the process of the quasi-super-resolution method. Actin filament fluctuation profiles were obtained from fluorescent images along with a single filament using the public-domain image processing program ImageJ (NIH). The x and y coordinates of the fluorescent profile peak of the actin filament were determined from the “plot profile” luminance distribution analysis tool in ImageJ. These coordinates were plotted on a 2-dimensional plane. A quadratic approximate curve was drawn from these coordinates because we assumed that there were no inflection points in the single actin filament. Fluctuations in the actin filaments were evaluated using this approximated curve.

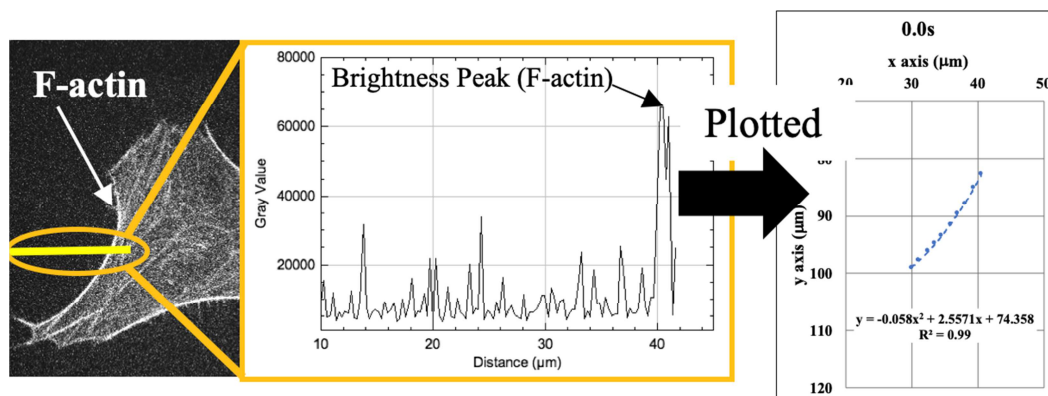


Figure 1. Coordinates of actin filaments were detected on the yellow line in fluorescence images. The actin filament is assumed to exit on the fluorescent peak as indicated by the arrow.

2.5. Analysis of Actin Filament Fluctuation Frequency in Network Structure

Actin filament fluctuations every 0.1 s were analyzed using the method described in a previous study [12]. This study analyzed the actin filament fluctuations every 0.1 s from 0 to 0.99 s (1) and (2) indicated the quadratic function curves of images that are adjacent in time.

$$f_1(x) = a_1x^2 + b_1x + c_1 \quad (1)$$

$$f_2(x) = a_2x^2 + b_2x + c_2 \quad (2)$$

From point B of $f_2(x)$, the normal line was calculated and drawn to $f_1(x)$, and the y-coordinate of point A was obtained, as shown in (3).

$$y = -\frac{1}{f_2'(p_2)}(x - p_2) + f_2(p_2) \quad (3)$$

The x-coordinate of point A, p_1 , was obtained as shown in (4):

$$\begin{cases} p_1 = \frac{-b' \pm \sqrt{b'^2 - 4a'c'}}{2a'} \\ a' = a_1 \\ b' = b_1 - \frac{1}{f_2'(p_2)}P_2 \\ c' = c_1 - f_2(p_2) - \frac{1}{f_2'(p_2)}P_2 \end{cases} \quad (4)$$

(5) shows the actin filament fluctuation amplitude every 0.1 s and the distance from observation point A to point B.

$$\text{Amplitude} = \sqrt{(p_2 - p_1)^2 + (f_2(p_2) - f_1(p_1))^2} \quad (5)$$

The frequency of actin filament fluctuations was determined by analyzing the amplitude of the actin filament fluctuations. In this study, we assumed that the pattern of actin filament fluctuations and the time required for one cycle of fluctuation had the same regularity. The cycle of actin filament fluctuation was determined by referring to the pattern of actin filament fluctuation at other times and the time taken for one fluctuation cycle. (6) shows the sum of the obtained amplitudes of the actin filament fluctuations divided by the number of data points n to obtain the average amplitude \bar{L} .

$$\bar{L} = \frac{L_1 + L_2 + L_3 + \dots + L_n}{n} \quad (6)$$

Figure 2 shows the amplitude calculations of the actin filament fluctuations every 0.1 s in quasi-super-resolution images, and the correlation of the fluctuations in the network were analyzed. (7) shows the interrelationships of the actin filament fluctuations analyzed by the fluctuation amplitudes of the actin filaments in the intracellular actin filament network structure. Because the direction of actin filament fluctuations varied, the interrelationship of actin filaments in the structure was evaluated by the correlation coefficients of the actin filament fluctuation amplitude every 0.1 s. The correlation coefficient r between the fluctuations of actin

filaments A and B was derived using (7). In (7), L_A is the amplitude of actin filament A fluctuation during 0.1 s, and \bar{L}_A is the average amplitude of the measured actin filament fluctuation during 10 s. L_B and \bar{L}_B were similar.

$$r = \frac{\sum_{i=1}^n (L_{Ai} - \bar{L}_A)(L_{Bi} - \bar{L}_B)}{\sqrt{\sum_{i=1}^n (L_{Ai} - \bar{L}_A)^2 (L_{Bi} - \bar{L}_B)^2}} \quad (7)$$

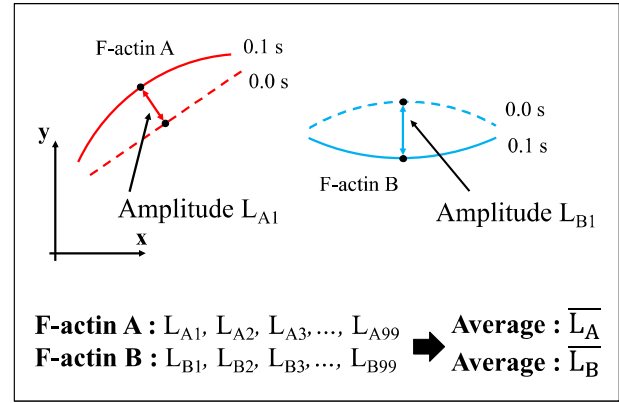


Figure 2. Correlation calculations of the actin filament fluctuation amplitude every 0.1 s. The averages of actin filament fluctuations were calculated from a dataset of 99 fluctuations. Amplitudes of 0.1 s were considered one data, regardless of the amplitude scale.

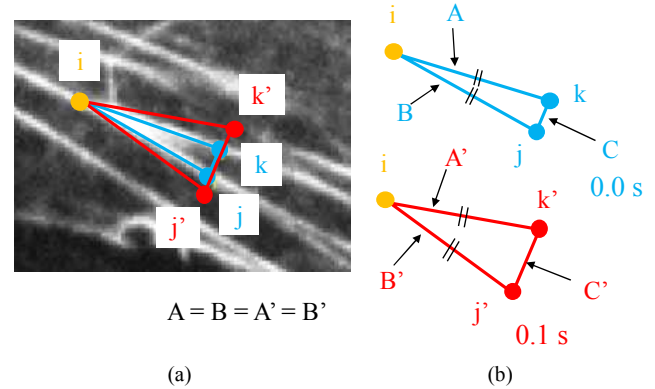


Figure 3. Analysis method of stress generated by actin filament fluctuations. The strain was evaluated from change of distance, c and c' .

2.6. Analysis of the Strain at the Connecting Point of Three Actin Filaments

The strain generated by the actin filament fluctuations at the connecting points was analyzed (Figure 3(a)). The strain was evaluated from the change in the distance between the observed points on the two actin filaments. Points k and j and k' , and j' were set on the actin filaments to be the same distance from point i (Figure 3(b)). The strain generated at the connecting point was evaluated from the distance C and C' that are between points k and j or k' and j' .

3. Result

Figure 4(a) shows a typical clear image of actin filaments in living NIH3T3 cells transfected with Lifeact-GFP for a 1 s exposure time. The developed actin filament network

structure was clearly observed, and the actin filaments were connected to each other. Figure 4(b) shows an image of the movie captured at 0.1 s intervals. The characteristics and numbers in Figure 4(b) were analyzed to determine the correlation between the fluctuations. Figure 5 shows a quasi-super-resolution image of actin filaments in living cells. The amplitudes of actin filament fluctuations were analyzed using approximate curves. Table 1 shows the maximum, minimum, and average amplitudes of the actin filament fluctuations for 10 s. The maximum and average amplitudes of the fluctuations near the central region of the cell were 0.99 μm and 0.27 μm , respectively. The maximum and average amplitudes of the fluctuations near the peripheral region of the

cell were 0.94 μm and 0.29 μm , respectively. Figures 6 and 7 show representative examples of changes in actin filament fluctuation amplitudes near the central and peripheral regions of the cell. Each actin filament fluctuation exhibited a different pattern. Table 2 lists the correlation coefficients of the amplitude of the actin filament fluctuation within the network structure. The maximum correlation coefficient was 0.2, indicating that there was no correlation between fluctuations among the many actin filaments in the network structure. As shown in Figure 4(b), the cell image is coarse, and the connecting points of the actin filaments are indistinct. It is difficult to analyze the strain at the connecting points.

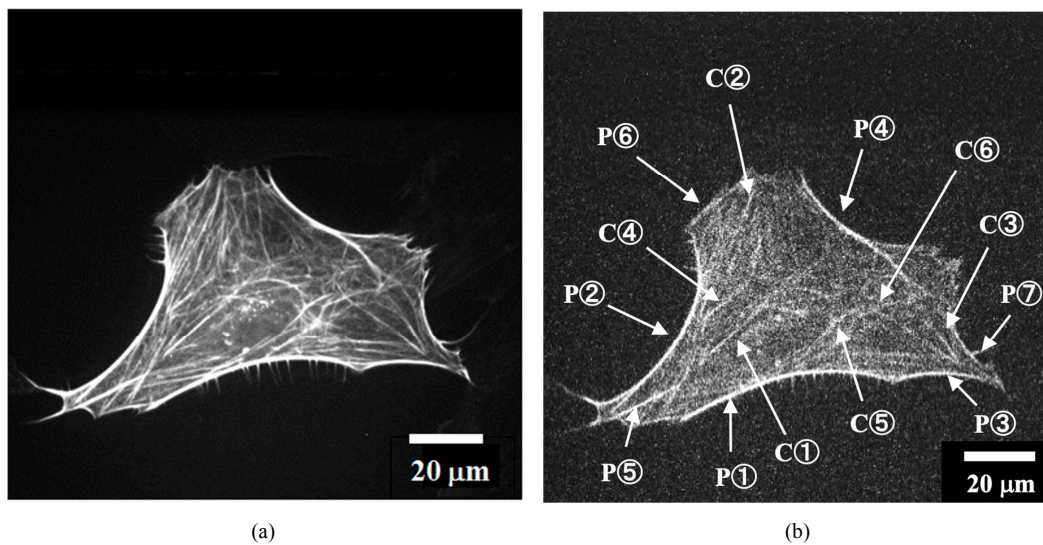


Figure 4. (a) Still image of actin filament network structure in a living cell at 37°C. (b) This image is from a movie captured at an interval of 0.1 s. Fluctuations in actin filaments indicated by arrows were analyzed.

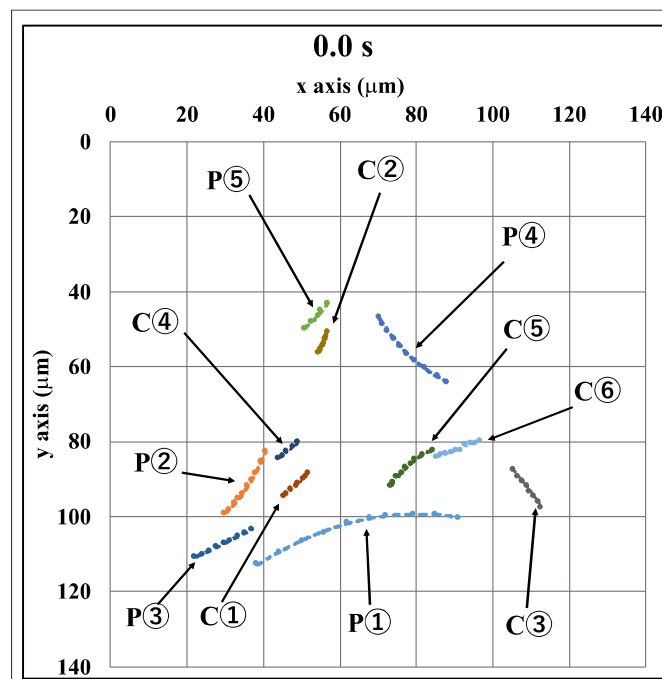


Figure 5. Typical quasi-super-resolution image of actin filaments network structure at 0 sec. Fluctuations in actin filaments were analyzed with quadratic functions of approximate curves.

Table 1. Maximum, minimum, and average of actin filament fluctuations.

Actin Filament Fluctuation Amplitude				
		Maximum Amplitude [μm]	Minimum Amplitude [μm]	Average [μm]
Center Region	C①	0.43	0	0.13
	C②	0.67	0	0.17
	C③	0.91	0	0.28
	C④	0.63	0	0.17
	C⑤	0.99	0	0.27
	C⑥	0.85	0	0.29
Peripheral Region	P①	0.47	0	0.16
	P②	0.26	0	0.07
	P③	0.32	0	0.08
	P④	0.94	0	0.29
	P⑤	0.86	0	0.21

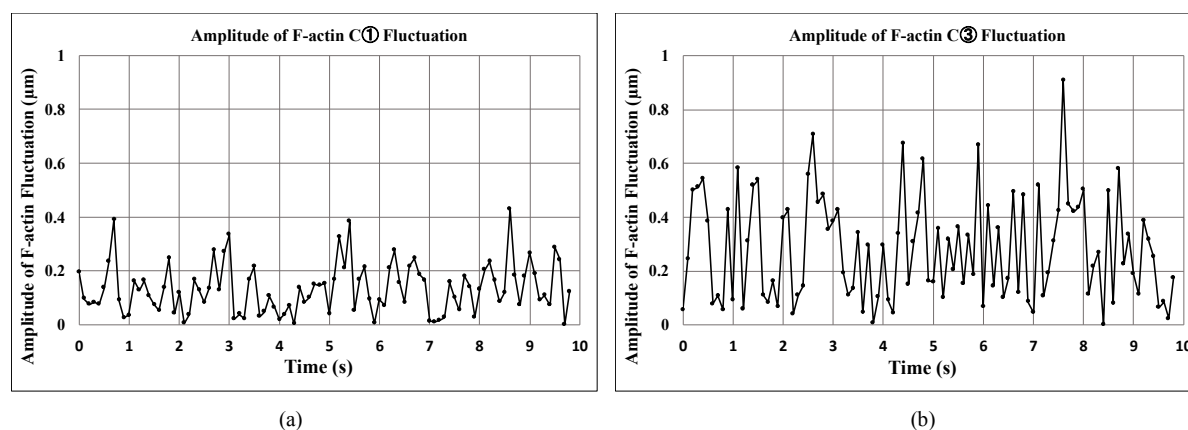


Figure 6. (a) Change in amplitude of actin filament C① fluctuations near the central region during 10 s. (b) Change in amplitude of actin filament C③ fluctuations near the central region during 10 s.

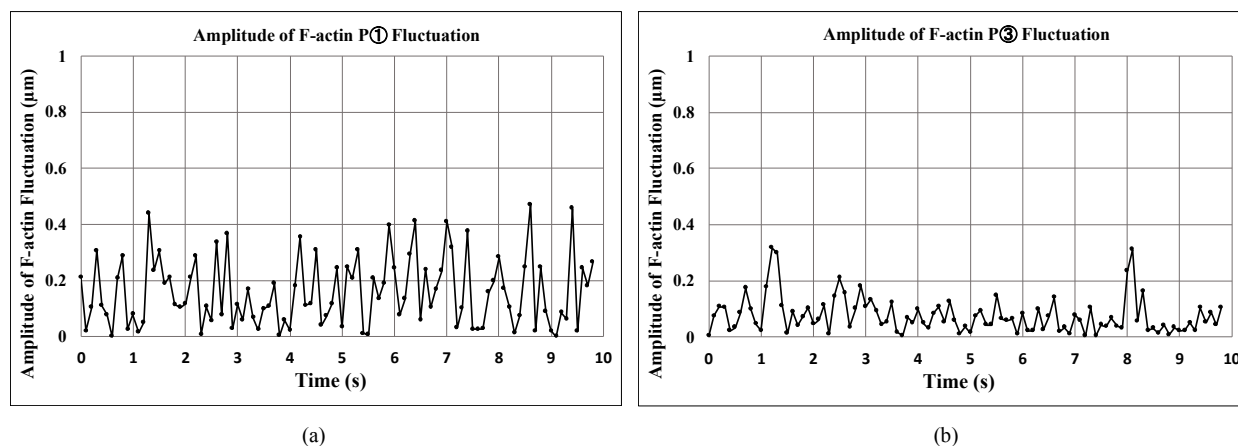


Figure 7. (a) Change in amplitude of actin filament P① fluctuations near the peripheral region during 10 s. (b) Change in amplitude of actin filament P③ fluctuations near the peripheral region during 10 s.

Table 2. Correlation coefficients of actin filament fluctuations.

[illegible]

Figure 8 shows the changes in the amplitude of the fluctuation at $y = 61.1 \mu\text{m}$ in a living cell observed in a previous study [9]. Table 3 lists the correlation coefficients of the actin filament amplitudes at $y = 51.1 \mu\text{m}$ and $y = 61.1 \mu\text{m}$. The observation coordinate at $y = 61.1 \mu\text{m}$ was near the midpoint and $y = 51.1 \mu\text{m}$ was near the end of the actin filament. Figure 9 shows actin filaments in other living

NIH3T3 cells. Actin filament fluctuations were analyzed, as indicated by arrows. Fluctuations near the midpoint of the actin filaments were analyzed. Table 4 lists the maximum, minimum, and average amplitudes of the actin filaments. The correlation coefficient of amplitude filament fluctuations was low (0.041).

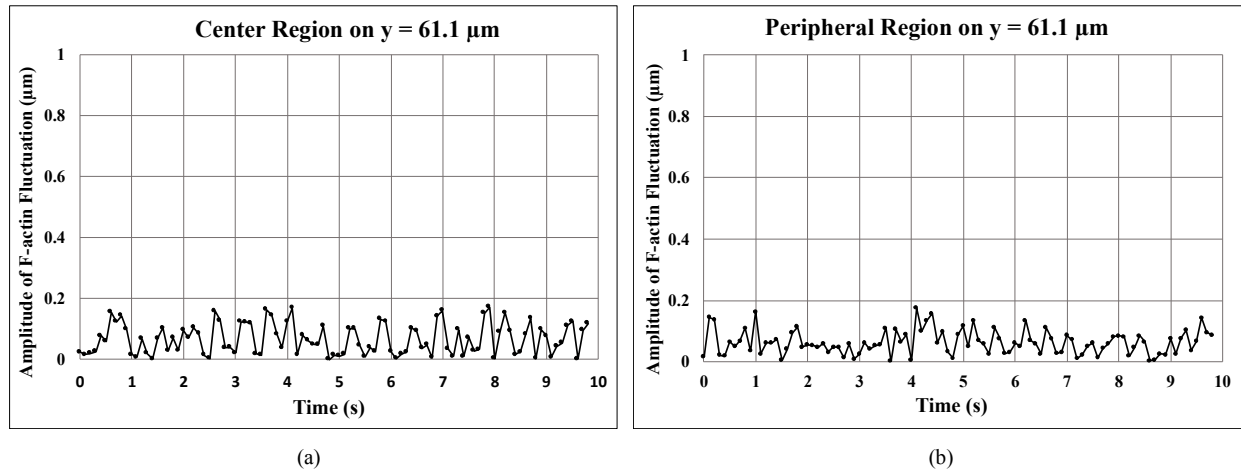


Figure 8. (a) Change of amplitude of actin filament fluctuation on $y = 61.1 \mu\text{m}$ near the central region during 10 s. (b) Change of amplitude of actin filament fluctuation $y = 61.1 \mu\text{m}$ near peripheral region during 10 s.

Table 3. Correlation coefficient of actin filament fluctuation amplitude at $y = 51.1 \mu\text{m}$ and $y = 61.1 \mu\text{m}$.

Correlation Coefficient of F-actin Fluctuation	
$y = 51.1 [\mu\text{m}]$	-0.03
$y = 61.1 [\mu\text{m}]$	0.14

Table 4. Maximum, minimum, and average of actin filament fluctuations.

Actin Filaments Fluctuation Amplitude			
	Maximum Amplitude [μm]	Minimum Amplitude [μm]	Average [μm]
Center Region	0.54	0	0.19
Peripheral Region	0.51	0	0.17

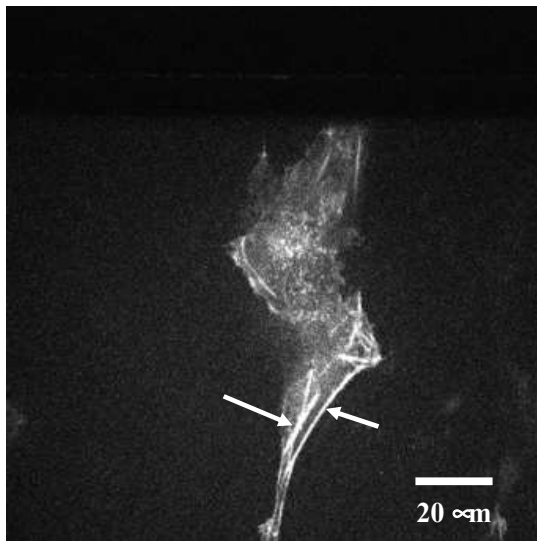


Figure 9. Still image of actin filaments near the central and peripheral regions of the cell at 37°C . Fluctuation of actin filaments indicated by arrows were analyzed.

In the other observed cells, actin fluctuations in the actin filament-connected area were analyzed, (Figure 10). The analyzed actin filaments are indicated by arrows in Figure 10. These actin filaments were clearly connected to each other. Figure 11 shows a quasi-super-resolution image of the actin filaments at 0.0 s. Table 5 lists the maximum, minimum, and average amplitude values of the actin filament fluctuation over 10 s, obtained using the quasi-super-resolution analysis method. Fluctuations were analyzed near the midpoint of the actin filaments. The maximum and average amplitudes of the fluctuations in actin filaments in the network structure were $0.78 \mu\text{m}$ and $0.21 \mu\text{m}$, respectively. Table 6 shows correlation coefficients of the amplitude of actin filament fluctuations in the network structure. The correlation coefficients of the amplitude of filament fluctuations were low, and there was no correlation with actin filament fluctuations. Figure 12 shows a quasi-super-resolution image at the connecting point of the three actin filaments at 10.8 s. Figure 13 shows the three observation points i, j, and k on the three actin filaments. The strain state was evaluated from the change in the distance

between points j and k starting from point i. Figure 14 shows the changes in the distance between j and k over 2 s. Figure 15 summarizes the changes in the direction of the observation

points between 0.1 s. The direction at each observation point changed randomly over a 2-s period.

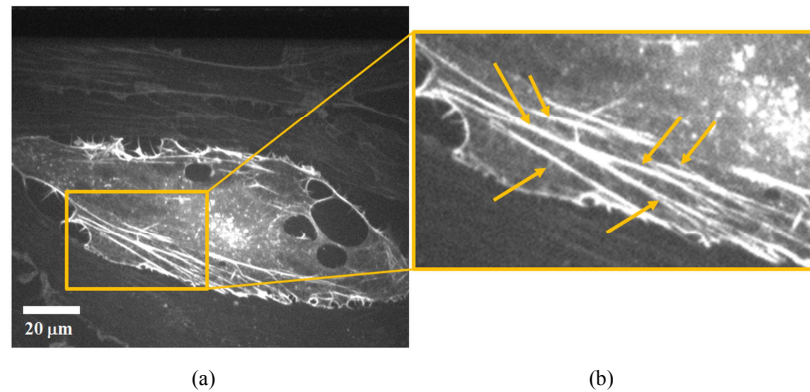


Figure 10. Fluorescent image of the actin filament network in living NIH3T3 cells at 37°C. Fluctuation in actin filaments indicated by arrows were analyzed.

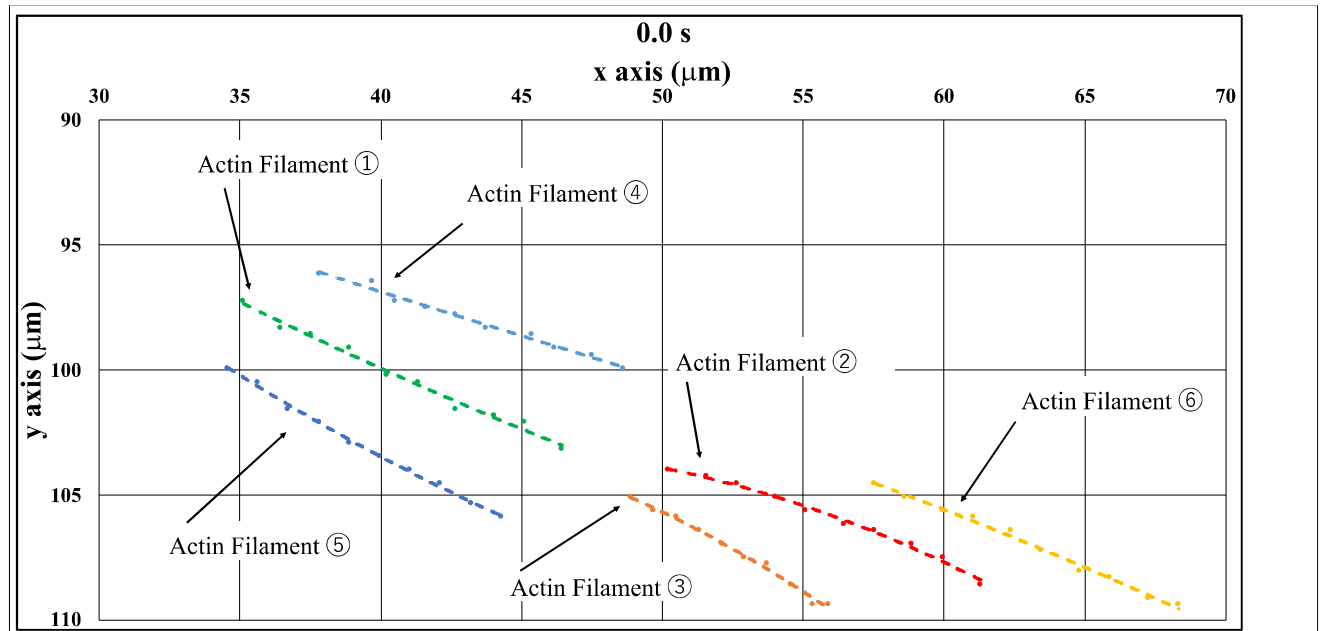


Figure 11. Quasi-super-resolution image of actin filaments in the network structure at 0 s. Actin filament fluctuations were analyzed with quadratic functions of approximate curves.

Table 5. Maximum, minimum, and average of the amplitude of actin filament fluctuations.

F-actin Fluctuation Amplitude			
	Maximum Amplitude [µm]	Minimum Amplitude [µm]	Average [µm]
F-actin ①	0.57	0	0.15
F-actin ②	0.48	0	0.15
F-actin ③	0.61	0	0.19
F-actin ④	0.57	0	0.20
F-actin ⑤	0.58	0	0.15
F-actin ⑥	0.78	0	0.21

Table 6. Correlation coefficients of actin filament fluctuations.

Correlation Coefficients of Actin Filaments Fluctuation					
	F-actin ②	F-actin ③	F-actin ④	F-actin ⑤	F-actin ⑥
F-actin ①	-0.09	0.08	0.09	-0.11	0.09
F-actin ②		-0.05	0.12	0.07	-0.02
F-actin ③			-0.29	0.05	0.04
F-actin ④				-0.01	-0.10
F-actin ⑤					-0.14

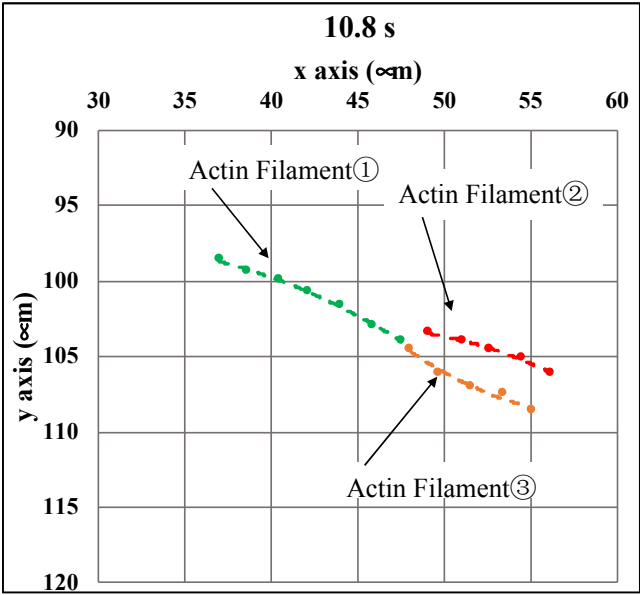


Figure 12. Quasi-super-resolution image of connecting point of actin filaments at 10.8 s.

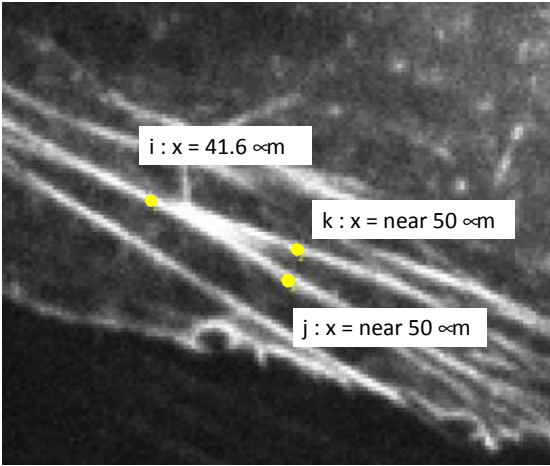


Figure 13. Observation points on three actin filaments of stress analysis. The strain generated by fluctuations in actin filaments was analyzed from changes in length between k and j.

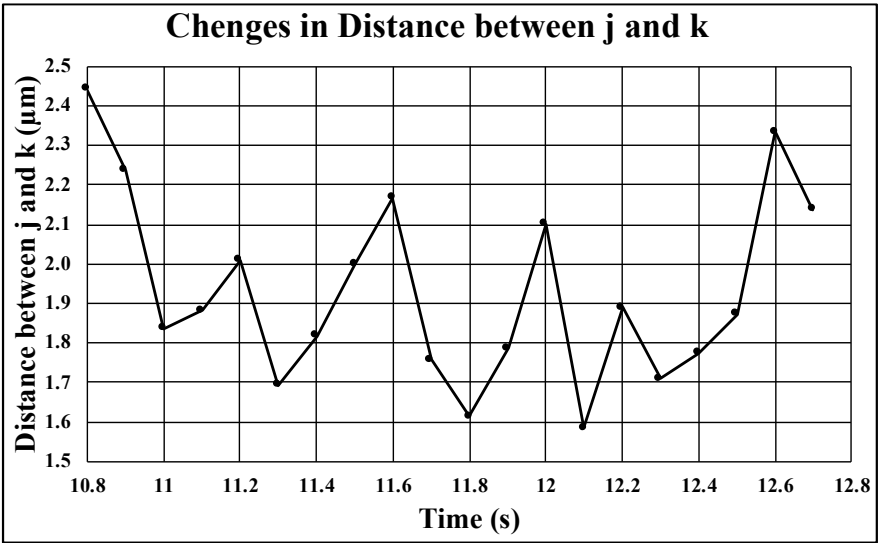


Figure 14. Change in strain generated by actin filament fluctuations. This strain change was analyzed for 2.0 s.



















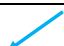



























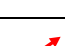







	Fluctuation Direction								
sec	10.9	11.0	11.1	11.2	11.3	11.4	11.5	11.6	11.7
Point i									
Point j									
Point k									
sec	11.8	11.9	12.0	12.1	12.2	12.3	12.4	12.5	12.6
Point i									
Point j									
Point k									

Figure 15. Rearrangement direction of observed points due to fluctuations every 0.1 s. The changes in rearrangement direction were random at each observation point.

4. Discussion

This study analyzed the actin filament network structures in living NIH3T3 cells transfected with Lifeact-GFP using quasi-super-resolution analysis. The quasi-super-resolution image analysis used in this study was our original methodology [9], and this method is effective for analyzing fast fluctuations in intracellular proteins. The observed fluctuations in the actin filaments near the central and peripheral regions of the cells were not uniform and randomly fluctuated without any correlation with each other. In addition, actin filament fluctuations near the central and peripheral regions of the cells were separately analyzed. No significant differences in the amplitude or pattern of actin filament fluctuations were found between the central and peripheral regions of the cell. In addition, the amplitude and pattern of fluctuation of actin filaments differed in each region. This difference was caused by differences in the structures surrounding the observed actin filaments and their tension [14]. The actin filaments observed in this study were limited by the spatial resolution of microscopy and differences in the expression levels and patterns of Lifeact-GFP. Therefore, the actin filaments observed in this study only refer to those that could be observed. Moreover, the structure of the intracellular actin filament network was developed in three dimensions. Different actin filament structures are believed to exist at the bottom and top of the cell. In the future, it will be necessary to analyze actin filament fluctuations and other protein structures in three dimensions.

No correlation was found between fluctuations in the respective actin filaments within the network structure. This suggests that actin filaments fluctuate independently of each other rather than throughout the network structure. Furthermore, we hypothesized that strain was generated by

disparate fluctuations in the actin filaments at the connecting points of the filaments. In Figure 13, the observation points i, j, and k are set near the connecting point in the acquired image. This structure was thought to comprise two actin filaments; however, because the structure could not be determined from the image, it was assumed to be connected by three actin filaments (Figure 12). The pattern of change in the distance between the observation points i and j in Figure 14 and the fluctuation directions of points i, j, and k in Figure 15 were random. This suggests that a randomly directed strain is generated by actin filament fluctuations at the connecting point, even when cells are under static culture conditions without any mechanical force application. Furthermore, this strain could also occur at protein complex structures, such as the LINC and the focal adhesion complex to which actin filaments and other cytoskeletons are connected. The fluctuation in intermediate filaments in living endothelial cells ceased when fluid shear stress was applied to the cells [15]. In this study, the acquisition rate of intermediate filament fluctuations in endothelial cells was considerably less than 1 Hz. This study suggests that fluctuations within the cytoskeleton temporarily disappear when cells are subjected to fluid shear stress, and that the strain generated by cytoskeletal fluctuations also disappears. This phenomenon, in which fluctuations in intracellular protein structures such as actin filaments stop and strain disappears within the protein network structure, is involved in the mechanism of cellular mechanosensing. We assumed that actin structures play a major role in the mechanosensing mechanisms of many types of cells. Therefore, to elucidate the mechanosensing mechanism of cells, it is important to observe the displacement and response of actin filaments immediately after the application of fluid shear stress. Furthermore, the observation of three-dimensional structural changes in actin filaments is important. Actin filaments are

connected to each other, the cell nucleus, and the focal adhesion complex at the bottom of the cells in three dimensions.

However, cytoskeletal structures comprising actin filaments and microtubules resemble tensegrity structures comprising elastic and compression forces [16]. In a future study, a tensegrity model that considers real cell dimensions, protein structure fluctuations, and physical properties of actin filaments [17, 18] and microtubules [19] will be developed. The stress caused by fluctuations in actin filaments in the cytoskeletal structure will be analyzed using this tensegrity model [20]. The properties of intracellular protein structures that change with the state of the protein structure [21] have been reported. Additionally, microtubules may fluctuate; therefore, various parameters should be determined with caution.

5. Conclusion

This study analyzed fluctuations in the actin filament network of living cells using a quasi-super-resolution analysis technique. The actin filaments in the network fluctuated independently, and a random strain was generated by the actin filament fluctuation at the connecting point. This strain is generated when cells are in static culture conditions, and flow shear stress is known to stop cytoskeletal fluctuations. These results suggest that the strain generated at the connecting point by fluctuations in actin filaments is in cellular mechanosensing.

Acknowledgments

This study was supported by a research grant from the Chairperson and President of Nihon University (2021–2022) and a JSPS KAKENHI Grant-in-Aid for Scientific Research(C), 21K12632.

References

- [1] Priyamvada Chugh, Andrew G. Clark, Matthew B. Smith, Davide A. D. Cassani, Kai Dierkes, Anan Ragab, Philippe P. Roux, Guillaume Charras, Guillaume Salbreux & Ewa K. Paluch. (2017). Actin Cortex Architecture Regulates Cell Surface Tension. *Nature Cell Biology* (6). doi: 10.1038/ncb3525.
- [2] Toshiro Anno, Naoya Sakamoto & Masaaki Sato. (2012). Role of Nesprin-1 in Nuclear Deformation in Cells under Static and Uniaxial Stretching Conditions. *Biochemical and Biophysical Research Communications* (1). doi: 10.1016/j.bbrc.2012.06.073.
- [3] Pakorn Kanchanawong, Gleb Shtengel, Ana M. Pasapera, Ericka B. Ramko, Michael W. Davidson, Harald F. Hess & Clare M. Waterman. (2010). Nanoscale Architecture of Integrin-Based Cell Adhesions. *Natures* (7323). doi: 10.1038/nature09621.
- [4] Laura M. Hoffman, Mark A. Smith, Christopher C. Jensen, Masaaki Yoshigi, Elizabeth Blankman, Katharine S. Ullman & Mary C. Beckerle. (2020). Mechanical Stress Triggers Nuclear Remodeling and the Formation of Transmembrane Actin Nuclear Lines with Associated Nuclear Pore Complexes. *Molecular Biology of the Cell* (16). doi: 10.1091/mbc.E19-01-0027.
- [5] Jason A. Mellad, Derek T. Warren & Catherine M. Shanahan. (2010). Nesprins LINC the Nucleus and Cytoskeleton. *Current Opinion in Cell Biology* (1). doi: 10.1016/j.ceb.2010.11.006.
- [6] Kazuaki Nagayama, Yuki Yahiro & Takeo Matsumoto. (2011). Stress Fibers Stabilize the Position of Intranuclear DNA through Mechanical Connection with the Nucleus in Vascular Smooth Muscle Cells. *FEBS Letters* (24). doi: 10.1016/j.febslet.2011.11.006.
- [7] Francis J. Alenghat & David E. Golan. (2013). Membrane Protein Dynamics and Functional Implications in Mammalian Cells. *Current Topics in Membranes*. doi: 10.1016/B978-0-12-417027-8.00003-9.
- [8] Carmine Di Rienzo, Vincenzo Piazza, Enrico Gratton, Fabio Beltram & Francesco Cardarelli. (2014). Probing Short-Range Protein Brownian Motion in the Cytoplasm of Living Cells. *Nature Communications* (5891). doi: 10.1038/ncomms6891.
- [9] Tomoteru Oka, Yasuyuki Oguma & Noriyuki Kataoka. (2022). Real-Time analysis of F-actin Fluctuation in Living Cells with Quasi Super-Resolution Technique. *Journal of Biomechanical Science and Engineering* (3). doi: 10.1299/jbse.22-00081.
- [10] Tai Kiuchi, Makio Higuchi, Akihiro Takamura, Masahiro Maruoka & Naoki Watanabe. (2015). Multitarget Super-Resolution Microscopy with High-density Labeling by Exchangeable Probes. *Nature Methods* (8). doi: 10.1038/nmeth.3466.
- [11] Toshihiro Sera, Marie Terada & Susumu Kudo. (2020). Heterogeneous Reorganization of Actin Filaments in Living Endothelial Cells in Response to Shear Stress. *Journal of Biorheology* (1). doi: 10.17106/jbr.34.18.
- [12] Hui Chen, Dilshad M. Choudhury & Susan W. Craig. (2006). Coincidence of Actin Filaments and Talin is Required to Activate Vinculin. *Journal of Biological Chemistry* (52). doi: 10.1074/jbc.M607324200.
- [13] Shigenobu Yonemura, Yuko Wada, Toshiyuki Watanabe, Akira Watanabe, Akira Nagafuchi & Mai Shibata. (2010). Alpha-Catenin as a Tension Transducer Induces Adherens Junction Development. *Nature Cell Biology* (6). doi: 10.1038/ncb2055.
- [14] Kandice Tanner, Aaron Boudreau, Mina J. Bissell & Sanjay Kumar. (2010). Dissecting Regional Variations in Stress Fiber Mechanics. In *Living Cell with Laser Nanosurgery*. *Biophysical Journal* (9). doi: 10.1016/j.bpj.2010.08.071.
- [15] Brian P. Helmke, Robert D. Goldman & Peter F. Davies. (2000). Rapid Displacement of Vimentin Intermediate Filaments in Living Endothelial Cells Exposed to Flow. *Circulation Research* (7). doi: 10.1161/01.res.86.7.745.
- [16] Ning Wang, James P. Butler & Donald E. Ingber. (1993). Mechanotransduction Across the Cell Surface and Through the Cytoskeleton. *Science* (5111). Doi: 10.1126/science.7684161.
- [17] Yuika Ueda, Daiki Matsunaga & Shinji Deguchi. (2022). A Statistical Mechanics Model for Determining the Length Distribution of Actin Filaments under Cellular Tensional Homeostasis. *Scientific Reports* (1). doi: 10.1038/s41598-022-18833-1.

- [18] Shinji Deguchi, Toshiro Ohashi & Masaaki Aato. (2006). Mechanical Properties of Stress Fiber in Adherent Vascular Cells Characterized by In Vitro Micromanipulation. *Future Medical Engineering Based on Bionanotechnology*. doi: org/10.1142/9781860948800_0007.
- [19] David B. Wells & Aleksei Aksimentiev. (2010). Mechanical Properties of a Complete Microtubule Revealed Through Molecular Dynamics Simulation. *Biophysical Journal* (2). doi: 10.1016/j.bpj.2010.04.038.
- [20] Gun S. Buntara. (2020). Computational Modeling of Tensegrity Structures. *Springer*.
- [21] Arif Md Rashedul Kabir, Daisuke Inoue, Yoshimi Hamano, Hiroyuki Mayama, Kazuki Sada & Akira Kakugo. (2014). Biomolecular Motor Modulates Mechanical Property of Microtubule. *Biomacromolecules* (5). doi: 10.1021/bm5001789.